World Academy of Science, Engineering and Technology
International Journal of Electrical and Computer Engineering
Vol:4, No:10, 2010

Design of Permanent Magnet Machines with Different Rotor Type

Tayfun Gundogdu, Guven Komurgoz

***Abstract*—** This paper presents design, analysis and comparison of the different rotor type permanent magnet machines. The presented machines are designed as having same geometrical dimensions and same materials for comparison. The main machine parameters of interior and exterior rotor type machines including eddy current effect, torque-speed characteristics and magnetic analysis are investigated using MAXWELL program. With this program, the components of the permanent magnet machines can be calculated with high accuracy. Six types of Permanent machines are compared with respect to their topology, size, magnetic field, air gap flux, voltage, torque, loss and efficiency. The analysis results demonstrate the effectiveness of the proposed machines design methodology. We believe that, this study will be a helpful resource in terms of examination and comparison of the basic structure and magnetic features of the PM (Permanent magnet) machines which have different rotor structure.

***Keywords*—** Motor design, Permanent Magnet, Finite-Element method.

I. Introduction

Electrical Machines are almost entirely used in producing electricity. New machine types play a considerable role in the distributed energy systems. In the past few years, many authors have devoted themselves to the different type designs of electrical systems. The PM machines has now commercial and importance of the PM upraises day after day because of the significant improvements in permanent magnets and power electronic devices and ever increasing need to develop smaller, cheaper and more energy-efficient motors. PM motors are not the most prevalent motor type in use at the present time. But, as their cost decreases, they will become a dominant motor type because of their compactness, high power density, fast dynamics, high torque to inertia ratio, drive and efficiency characteristics [1]. The first PM excitation systems were applied to electrical machines as early as the 19th century, e.g., J. Henry (1831), H. Pixii (1832), W. Ritchie (1833), F. Watkins (1835), T. Davenport (1837), M.H. Jacobi (1839) [2]. There are a lot of different PM constructions which are changed according to the use of the motor (constant torque, constant speed, constant power and etc.). And also these motors have interior and exterior rotor types.

The recent studies in open literature indicate that many researchers and engineers have started working on design of PM machines. The analysis of different PM machines for hybrid electric vehicles application was investigated by Dajaku and Gerling. In this study, machine parameters, electromagnetic torque and the skewing effect are investigated using ANSYS program [3]. The design of a 20000 rpm, 3-phase brushless permanent magnet DC motor for use in a friction welding unit, in which studs up to 3 mm diameter are welded by coordinating the rotational speed of the motor with the force applied by a linear permanent magnet servo-actuator, was designed by Zhu et al.[4]. A finite-element analysis of the electromechanical field of a BLDC motor considering speed control and mechanical flexibility was presented by Jang et al. [5]. In this study, the magnetic field is analyzed by the nonlinear time-stepping finite-element method considering the switching action of the pulse width modulation inverter. A new approach to the optimized design of a surface-mounted PM brushless DC motor was investigated by Bianchi and et al. [6]. The other studies, analytical calculation, modeling and optimization of the permanent magnet motors was investigated and simulated. [7]-[10].

In this study, interior and exterior type PMDCMs (permanent magnet dc motors) are investigated according to constant dimensions, materials and power to make comparison between different design. To do this the MAXWELL program is employed and the same dimensions such as, size and number of slots, outer and inner diameters, type of permanent magnet, etc. are used in all types of the PMDCMs. That means a geometric analysis was performed. On the other hand, there are many studies on PMs which have various types of rotor geometry. But none of them have taken into account to comparison of magnet geometries (various rotor types) as the present study does.

II. Permanent Magnet Machines

The use of PMs in construction of electrical machines brings the following benefits [11]:

1) No electrical energy is absorbed by the field excitation system and thus there are no excitation losses which means substantial increase in the efficiency,
2) Higher torque and/or output power per volume than when using electromagnetic excitation,
3) Better dynamic performance than motors with electromagnetic excitation,

T. G. is a Researcher Assistant in the Istanbul Technical University, Faculty of Electrical and Electronics, Maslak, 80626, Istanbul, Turkey (corresponding author to provide phone: +90 505 809 2225; e-mail: tayfun.gundogdu@gmail.com).

G. K. is an Ass. Prof. Dr. in the Istanbul Technical University, Faculty of Electrical and Electronics, Maslak, 80626, Istanbul, Turkey (e-mail: komurgoz@itu.edu.tr).

4) Simplification of construction and maintenance,
5) Reduction of prices for some types of machines.

The stator of a PM machine has a conventional three-phase winding, and the rotor can have magnets mounted on the surface of the rotor, or there can be magnets buried inside the rotor [3]. In PM brushless motors the power losses are practically all in the stator where heat can be easily transferred through the ribbed frame or, in larger machines. These motors are used extensively where precise speed control is necessary, as electric radio-controlled vehicles, in computer disk drives or in video cassette recorders, the spindles within CD, CD-ROM drives, in industrial robots, in the robotic arms, and mechanisms within office products such as fans, laser printers and photocopiers in commonly used.

A. Permanent Magnets

A PM can produce magnetic field in an air gap with no excitation winding and no dissipation of electric power. External energy is involved only in changing the energy of magnetic field, not in maintaining it. As any other ferromagnetic material, a PM can be described by its B-H hysteresis loop. PMs are also called hard magnetic materials, meaning ferromagnetic materials with a wide hysteresis loop. There are three classes of PMs currently used for electric motors [11]:

1) Alnicos (Al, Ni, CO, Fe);
2) Ceramics (ferrites), e.g., barium ferrite BaOx6Fez03 and strontium
3) Rare-earth materials, i.e., samarium-cobalt SmCo and neodymiumferrite SrOx6Fez03; iron-boron NdFeB.

B. Location of the Permanent Magnets

Figure 1 shows six basic conFigurations of the PM machines. Mainly, the magnets could be placed on the

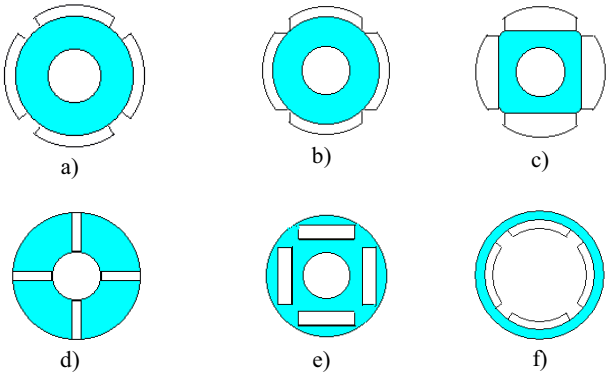

Fig. 1 Different rotor construction of a PM machines; a) Surface mounted magnets-vertical to shaft, b) Surface mounted magnets-parallel to shaft, c) Surface mounted magnets d) Buried radial magnets, e) Buried tangential magnets, f) PM machine outer rotor [12].

rotor surfaces or buried in the rotor. The rotor construction and location of the permanent magnets have a considerable effect on the motor properties. The interior construction simplifies the assembly and relieves the problem of retaining the magnets against centrifugal force. It also permits the use of rectangular instead of arc shaped magnets, and usually there is an appreciable reluctance torque which leads to a wide speed range at constant power.

III. Mathematical Modeling

The analysis and control of electrical machines requires an accurate mathematical model for performance assessment and system simulation. PM motor operates converting electrical energy to magnetic and then to mechanical energy. Magnetic energy plays an important role in the production of torque. So it is necessary to formulate magnetic field. The time-dependent magnetic equation is expressed as:

$$\nabla v \nabla A = J_s - \sigma \frac{\partial A}{\partial t} - \sigma\ V \nabla\ + \nabla d V \nabla A \qquad (1)$$

Where H_c is the coercivity of the permanent magnet, v is the velocity of the moving parts, A is the magnetic vector potential, V is the electric potential, J_s is the source current density, σ is the reluctivity.

The transient solver applies a reference frame that is fixed with respect to the components in the model by setting the velocity, v, equal to zero. This is possible by considering the equation for the magnetic vector potential both in moving part and stationary part in their own reference frame in which velocity is always zero. Because the moving components have now been fixed to their own coordinate system, the partial time derivative becomes the total time derivative of A. Thus, the motion equation becomes [13]:

$$\nabla v \nabla A = J_s - \sigma \frac{\partial A}{\partial t} - \sigma\ V \nabla\ + \nabla_c\ H \qquad (2)$$

IV. Analysis of PM Machines using FEM

Detailed knowledge of the field distribution in the air gap of PM motor is of great importance for accurate prediction torque and efficiency characterizes. Magnetic field distribution can be found analytically for very simple geometries. In most cases, the magnetic field distribution can be obtained using some numerical methods such as Finite Element Method (FEM), Finite Difference Method (FDM), Boundary Element Method (BEM).

By using FEM, it is possible to make the accurate field calculations in the electrical machines. FEM produces the most accurate results if the geometric discritazation is fine enough. FEM allows accurate determination of machine parameters through magnetic field solutions as it takes into account the actual distribution of the winding, details of geometry, and the non-linearity of the magnetic materials of an electrical machine. The machine parameters and the electromagnetic torque are very important considerations for both analysis and design of electrical machines.

In this study, magnetic examination of the designed brushless permanent magnet DC motors according to iron sheet package structure was performed with Maxwell 2D program. From this electromagnetic analysis, actual potential

magnetic flux intensity of the motor was obtained. The simulation was completed following steps;

1) Create the geometric model
2) Assign materials to objects in the structure
3) Determination of the boundary conditions and mesh operation
4) Define the desired sources (electromagnetic excitations) and boundary conditions for the model
5) Compute other quantities of interest during the solution process. Quantities include forces, torques, matrices, or flux linkage
6) Compute the desired field solution and any requested parameters (force, torque, and so forth)
7) Solve to generate the solutions
8) View the results

V. Motor Geometry

A. Parameters of designed PM machines

In this work, twelve-poled rotor nub made up by NdFeB magnet material and stator nub with 36 slots coiled on copper conductor and spindle are used for all types of the designed motors. All analysis was performed according to constant power, so the rate of change of the rated motor rpm is between 197 and 224. Dimensions of the designed motors are determined according to current type, rated speed, motor coefficient and power density of the motor. General geometries of the motors are shown in Fig. 2. and Fig. 3.

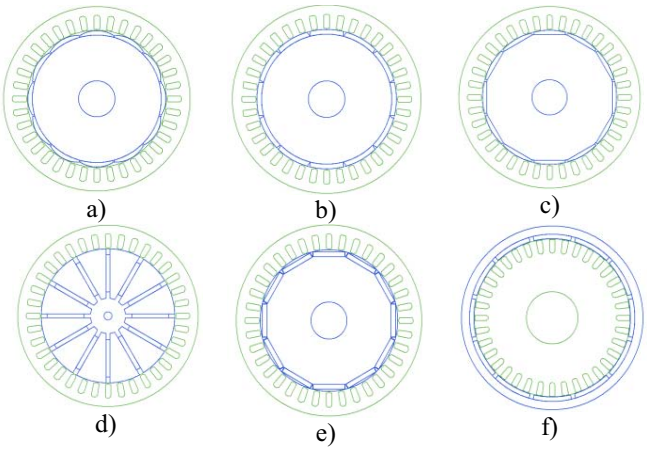

Fig. 2 Overwiev of designed motors.

Rated values, geometric stator and rotor parameters of the designed machines are given in Table I-III.

TABLE I
Parameters of all the designed machines

Rated Output Power (kW)	0.16
Rated Voltage (V)	24
Number of Poles	12
Given Rated Speed (rpm)	160
Frictional Loss (W)	1,88235
Windage Loss (W)	0.833706
Rotor Position	Inner
Type of Load	Constant Power
Operating Temperature (°C)	75

TABLE II
Geometric stator parameters

Number of Stator Slots	36
Outer Diameter of Stator (mm)	202
Inner Diameter of Stator (mm)	150
Length of Stator Core (mm)	66
Stacking Factor of Stator Core	0.97
Type of Steel	Steel_1008

Different magnetic materials selected for different parts of the motor are presented in Table IV.

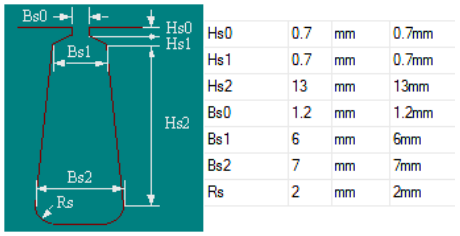

Fig. 3. Slot geometry of the stator

TABLE III
Geometric Rotor parameters

Air Gap (mm)	0.6
Inner Diameter (mm)	40
Length of Rotor (mm)	66
Stacking Factor of Iron Core	0.97
Type of Steel	Steel 1008
Mechanical Pole Embrace	0.92
Electrical Pole Embrace	0.934872
Max. Thickness of Magnet (mm)	5
Width of Magnet (mm)	35,6846
Type of Magnet	NdFeB35

TABLE IV
Magnetic materials used in Designed PM machines

Stator (Lamination)	Steel_1008B-H curve
Rotor (Lamination)	Steel_1008 B-H curve
Stator conductor type	Copper
Permanent magnet	NdFeB35 B-H curve
Air gap	Air (0.6 *mm*)
Spindle	Stainless steel

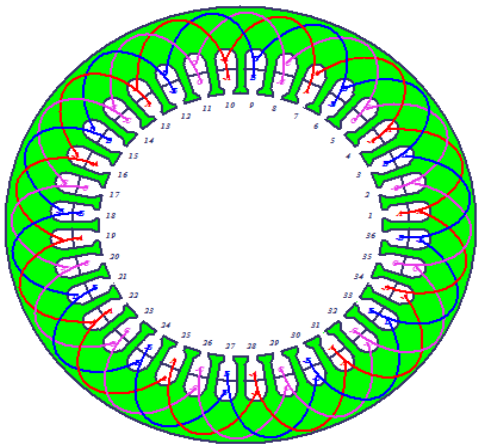

Fig. 4 Stator and coil structure of the designed motors

B. Winding Topologies

The operation principle of electric machines is based on the interaction between the magnetic fields and the currents

flowing in the windings of the machine. In this study, the distributed type windings are used in the all types of designed machines. It is desired that the MMF (magneto-motive force) produced by stator windings to be as sinusoidal as possible.

The number of the phases in the motors designed in this study is three and each of the phase coils include 40 turns conductor. The number of the poles in the design is 12, and the number of the slots was determined to be 36. The coils are in the form of two-storey (two bobbin edges per slot), yet they are in the form of concentric coil. In Fig. 4, stator coils and the structure of layered mounting coil can be seen as well.

C. Driver Circuit of the designed machines

These motors are driven by a circuit consisting of 6 transistors. The acquired square wave shapes can feed the stator without causing any breakdown. During each commutation, first coil is energized with positive power, second coil is negative and the third coil is in the state of not energized [14].

Acquired DC energy feeds two motor coils at 10˚ periods. During that time, the third coil does not carry current and it is in the position without energy. At the end of each 10˚ period, the current changes its direction from one of the conducting lines towards unloaded line. Lead angle of trigger in electric degrees and trigger pulse width in electric degrees of the designed motors are 10˚ and 120˚ respectively.

VI. Results and Discussion

The machine parameters and the electromagnetic torque are very important considerations for both analysis and design of electrical machines. Magnetic examination of the designed brushless PMDCMs according to iron sheet package structure with the same magnet dimensions used in all the designed motors was performed (as given Fig. 5). The results of the simulations were analyzed through curves and graphics. These curves and analysis results are presented in Fig. 6-10 and Table V respectively.

From this electromagnetic analysis, actual potential magnetic flux intensity of the motor was obtained. They showed that the rated working borders are within the acceptable levels. Flux lines of the designed machines are shown in the Fig .5.

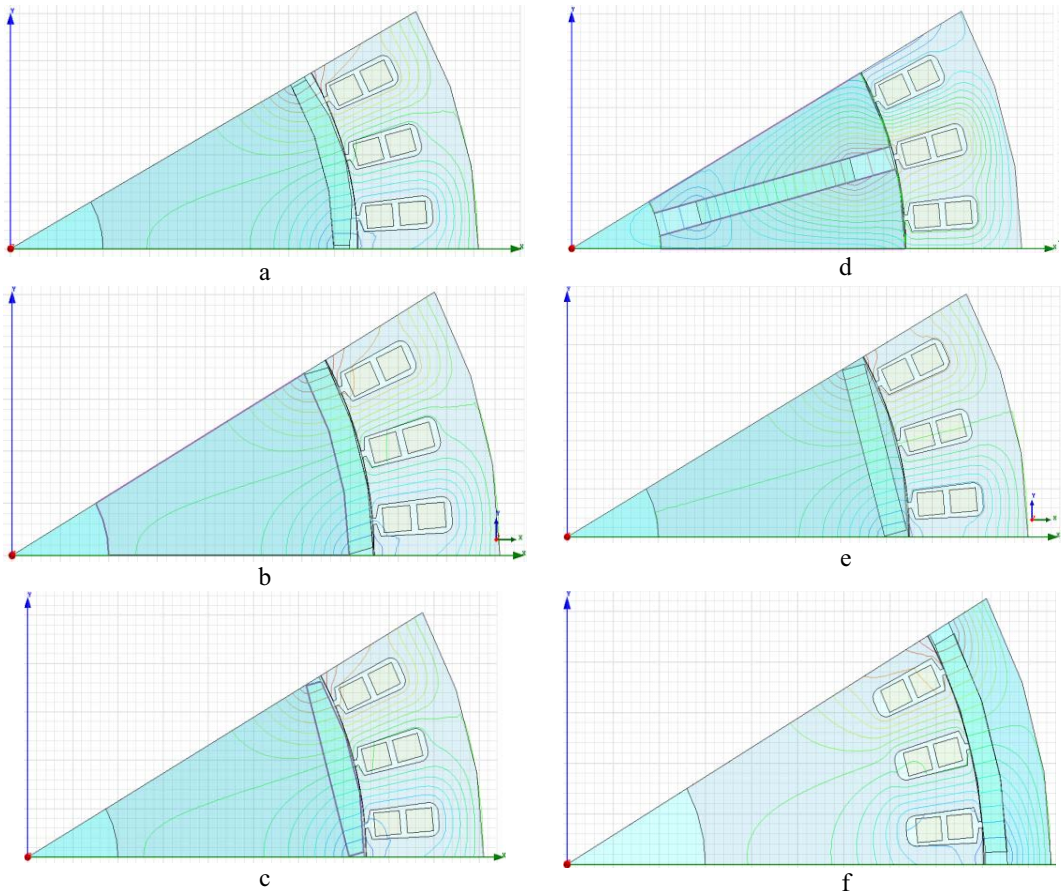

Fig. 5. Flux lines of the designed machines.

According to speed and efficiency, the a type motor is better than the others (Table V). According to rated torque, the d and f types motors are better that the others. From the B/H characteristic curves of NdFeB magnet used for rotor and steel 1008 used for stator, it can be seen that, Steel 1008 and NdFeB magnet has a saturation point at 2–2.30 T and 1,23 T respectively. That is meant that, motors never work at saturation point except f type. In the magnetic analysis conducted with Maxwell 2D, no-load operation flux density of designed motors was found as shown in Table VI. Flux

line distributions pass over stator and rotor and through the air gap. This shows that the designed motor works at appropriate air gap. The performance curves of the designed motors show that rated working gaps are at the acceptable levels.

TABLE V
ANALYSIS RESULTS OF THE SIX MOTORS

Feature\Motor Type	a	b	c	d	e	f
Total Net Weight (kg)	15,744	15,851	15,844	15,327	15,905	15,712
Rated Speed (rpm)	220,69	224,71	223,18	196,8	266,81	212,04
Rated Torque (N.m)	6,9305	6,8066	6,8510	7,7646	5,7260	7,2063
Total Loss (W)	34,618	34,961	34,755	34,626	58,271	50,224
Output Power (W)	160,17	160,17	160,11	160,02	159,98	160,01
Input Power (W)	194,79	195,13	194,87	194,64	218,26	210,24
Efficiency (%)	82,228	82,083	82,165	82,210	73,301	76,111

TABLE VI
NO-LOAD MAGNETIC DATA

Magnetic Data	a	b	c	d	e	f
Stator-Teeth B (T)	2,028	1,894	1,931	2,046	0,488	2,092
Stator-Yoke B (T)	1,897	1,890	1,944	2,051	0,451	0,473
Rotor-Yoke B (T)	0,391	0,410	0,401	0,384	0,084	2,17
Air-Gap B (T)	1,164	1,074	1,099	1,161	1,027	0,955
Magnet B (T)	1,039	1,112	1,089	0,809	1,214	0,945

In the d type motor, the magnets appear orthogonal to the air gap, rather than facing it, and the magnet flux is directed to the air gap through electrical steel. The primary reason for this structure is that flux concentration is possible if the surface area of the magnets exceeds that of the block of steel at the air gap. This conFiguration is popular when higher performance is desired when using inexpensive ferrite magnets. As it is seen in Fig. 6, air gap flux intensity of the brushless DC motor is in the form of isosceles trapezoid.

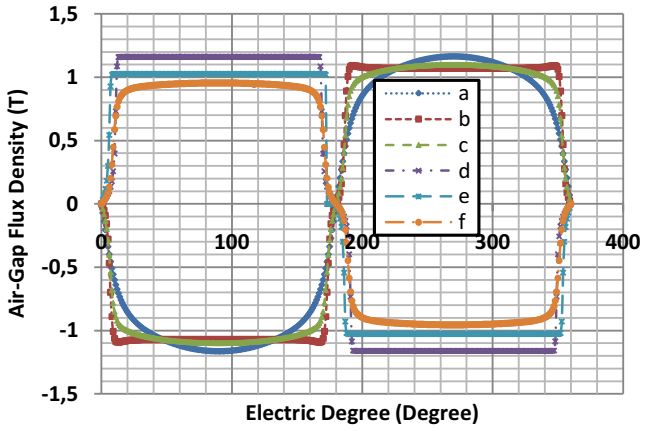

Fig. 6 Air gap flux intensity curve of the designed motors.

As it is seen in Fig. 7 and (3); while motor is starting, excessive current is driven from the network because starting speed is zero, so IR is maximum and I is also maximum. When motors reach the rated speed, they draw approximately 8 A. Speed-current range of the b type motor is larger than the others.

$$n = \frac{30}{\pi}\left(\frac{V_0 - I\ R}{k_e}\right) \tag{3}$$

The speed of the machine according basic equivalent motor circuit is given in (3). Where, V_0 is input voltage, I is input current, R is armature resistance, k_e EMF constant of the motor, n is speed.

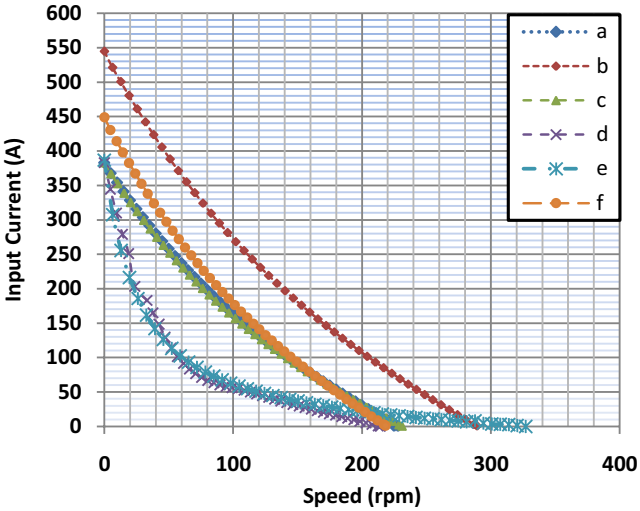

Fig. 7 Input current-speed graph of the designed motors.

The efficiency of the motor can be defined as follows;

$$\eta = \frac{P_{out}}{P_{in}} \tag{4}$$

As it is seen in (4), input power is proportional to input voltage, output power is proportional to speed. In Fig. 8, it is seen that output power-speed range of the b type motor is larger than the other motors. The b type motor can use in the application which requires large output power-speed range.

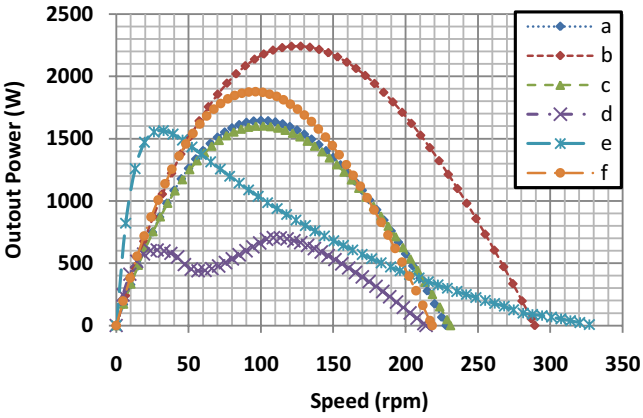

Fig. 8. Output power-speed graph of the designed motors.

In Fig. 9, efficiency-speed graph of the designed motor is shown. The efficiency of a motor depends with the ratio of output power and input power. The f and c type motors have almost same efficiency-speed ratio. The e type motor has very large efficiency-speed ratio. c, d and f type motors have average efficiency-speed ratio.

In Fig. 10, the torque-speed graph of the designed motor is shown. As it is mentioned before, torque and speed are

inversly proportional to each other. It is seen that the torque-speed graph of the a,b,c and f types of motors are linear.

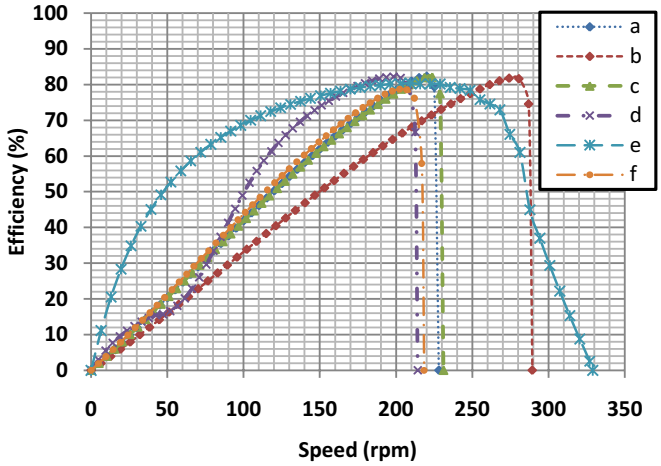

Fig. 9. Efficiency-speed graph of the designed motors.

Linearity of the torque-speed curve of a motor is important for stable operation. So, a,b,c and f types of motors are always stable but, d and e types of motors are stable after 50 rpm. The torque ripple can be minimized both by the proper motor design and motor control. Measures taken to minimize the torque ripple by motor design include elimination of slots, skewed slots, special shape slots, selection of the number of stator slots with respect to the number of poles, decentered magnets, skewed magnets, shifted magnet segments, selection of magnet width, direction-dependent magnetization of PMs [15].

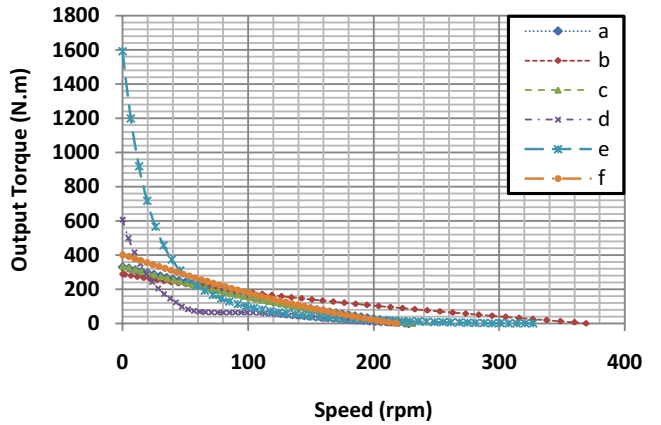

Fig. 10. Torque-speed graph of the designed motors.

VII. Conclusion

In this paper, the general and magnetic performances of PM machines with interior and exterior rotor types are investigated using finite element method. The main model parameters are analyzed using MAXWELL program. Six types PM machines are also compared with respect to their topology, size, magnetic field, air gap flux, voltage, torque, loss, and efficiency. After simulations we realized that, the efficiency of the f type motor is fewer that the others because of the stator slot shape.

References

[1] D. C. Hanselman, *Brushless Permanent-Magnet Motor Design*. New York: McGraw-Hill, 1994 ch. 5
[2] "B. B. Philips Techn Review" 35(4): 77-95, 1975.
[3] G. Dajaku and D. Gerling, "Design of Permanent Magnet Machines for Hybrid Vehicles," ANSYS Conference & 25th CADFEM Users' Meeting 2007.
[4] Z.Q. Zhu, K. Ng, and D. Howe, "Design and Analysis of High-Speed Brushless Permanent Magnet motors," Eighth International Conference on Electrical Machines and Drives 1-3 Sept. 1997, p.381–385.
[5] G. H. Jang, J. H. Chang, D. P. Hong, and K. S. Kim, "Finite-Element Analysis of an Electromechanical Field of a BLDC Motor Considering Speed Control and Mechanical Flexibility," IEEE Transactıons On Magnetıcs, Vol. 38, No. 2, March 2002.
[6] N. Bianchi and S. Bolognani, " Electrical Machines and Drives," IEEE Eighth International Conference (Conf. Publ. No. 444), 1997
[7] A. Marino, "Analytical Modeling and Optimization of a Radial Permanent Magnets Synchronous Machine," LEROY-SOMER, France.
[8] J. H. Seoa, S. Y. Kwaka, T. K. Chungb, S. Y. Jungc and H. K. Junga, "Optimal design of interior-permanent magnet synchronous machine for vehicle using improved niching genetic algorithm," International Journal of Applied Electromagnetics and Mechanics 29 (2009), pp 37–45,2009.
[9] S.R. Holm , H. Polinder, J.A. Ferreira, M.J. Hoeijmakers, P. van Gelder and R. Dill, "Analytical Calculation of the Magnetic Field in Electrical Machines due to the Current Density in an Airgap Winding," Proc. International Conference on Electrical Machines (ICEM 1996), pp. 348–352.
[10] D. Zarko, D. Ban, and T. A. Lipo, "Analytical Calculation of Magnetic Field Distribution in the Slotted Air Gap of a Surface Permanent-Magnet Motor Using Complex Relative Air-Gap Permeance," IEEE Transactions On Magnetics, Vol. 42, No. 7, July 2006.
[11] J. F. Gieras, *Permanent Magnet Motor Technology Design And Applications*. Second Edition, Revised And Expanded, New York: Marcel Dekker, 2002, ch. 1.
[12] Ansoft Maxwell RMxprt Program, Version 12.2.0, 1989-2009 Ansoft LLC.
[13] Ansoft Maxwell Online Help,Version 12.2.0, 1989-2009 Ansoft LLC.
[14] *Brushless DC (BLDC) Motor Fundamentals. – Microchip,* Pedmarja Yedamale Microchip Technology Inc. – 2003.
[15] B. J. Brunsbach, G. Henneberger, T. Klepach "Compensation of torque ripple," Int. Conf. ICEM'98, Istanbul, Turkey, 1998, pp. 588-593.,

T. Gundogdu completed his BS (2009) in electrical education at the Gazi University. He is working as a researcher assistant in the electrical engineering department at the Istanbul Technical University. He is interested in Design of Electrical Machines, Power Electronics, Artificial Neural Networks, and Microcontrollers.

G. Komurgoz completed her BS (1991), MS (1995), and PhD (2002) all in electrical engineering at the Istanbul Technical University. She is currently an assistant professor of electrical engineering. She is interested in Heat Transfer, Numerical Methods, Design of Transformer and Electrical Machines.